EUROPEAN ORGANIZATION FOR NUCLEAR RESEARCH

CERN-PPE/96-50
April 3, 1996

Search For New Particles In Hadronic Events With Isolated Photons

L3 Collaboration

Abstract

A search for the neutral Higgs boson in the processes $e^+e^- \to Z \to H^0\gamma \to q\bar{q}\gamma$ and $e^+e^- \to Z \to Z^*H^0 \to q\bar{q}\gamma\gamma$ has been performed using 2.8 million hadronic Z decays collected with the L3 detector at LEP from 1991 through 1994. No evidence for these processes has been observed. Upper limits at 95% confidence level for the corresponding cross sections have been set and the results have been compared with theoretical predictions beyond the Standard Model.

Submitted to *Phys. Lett. B*

Introduction

The minimal version of the Standard Model (SM) [1] predicts the existence of a neutral Higgs boson H^0 [2] with an unknown mass. At LEP, a H^0 lighter than the Z could be observable through the processes

$$e^+e^- \to Z \to H^0\gamma, \qquad H^0 \to q\bar{q}, \tag{1}$$

and

$$e^+e^- \to Z \to H^0Z^*, \qquad H^0 \to \gamma\gamma, \qquad Z^* \to q\bar{q}. \tag{2}$$

In the SM, reaction (1) occurs at the one-loop level with charged particles inside the loop, the dominant contribution coming from the $W^\pm$ bosons (Figure 1a). The fermion contributions are negligible due to the lower masses involved. Process (2) is also suppressed in the SM framework, since the H^0 decay into two photons proceeds via a similar loop-diagram (Figure 1b). Within the SM the cross section for process (1) is below 0.1 pb and for process (2) below 10^{-2} pb.

However, in several extensions of the Standard Model, these branching ratios can be significantly enhanced. For example in the Minimal Supersymmetric Standard Model (MSSM) the loop-diagrams of processes (1) and (2) may contain supersymmetric particles (e.g. charginos), resulting in branching ratios which can be increased by up to a factor of 3 [3,4].

A non-standard symmetry breaking may also lead to anomalous interactions of the Higgs with the electroweak gauge bosons affecting the Higgs production and decay mechanisms. The anomalous interactions can be described by an effective dimension-six Lagrangian $\mathcal{L}_{\text{eff}} = \sum_1^7 \frac{f_i}{\Lambda^2}\mathcal{O}_i$, where $\mathcal{O}_i$ are the operators representing the anomalous couplings, Λ is the typical energy scale of the interactions and f_i are constants defining the strength of each term [5]. Whereas in the SM the decay $H^0 \to \gamma\gamma$ occurs at the one-loop level, dimension-six operators contribute at the tree level and can therefore lead to large deviations from the SM. Low energy experiments provide a measurement of some of the coefficients f_i/Λ^2, typical values being of $O(1\ \text{TeV}^{-2})$ with some of them being as large as $O(100\ \text{TeV}^{-2})$. The decay width $\Gamma(H^0 \to \gamma\gamma) \propto (f_i/\Lambda^2)^2$, and for some combinations of the coefficients the branching ratio $\Gamma(H^0 \to \gamma\gamma)$ can be enhanced by a factor as large as 10^4 [5]. Similarly, the decay $Z \to H^0\gamma$ (one-loop level in the SM) is sensitive to such anomalous couplings and can therefore be largely enhanced by the dimension-six contributions occurring at the tree level.

In addition, in some composite models like the Strongly-Coupled Standard Model (SCSM) the branching ratios for reactions (1) and (2) can differ from the SM values [6,7]. Assuming a scale factor Λ characterising the SCSM interaction to be about 300 GeV, the branching ratio $\Gamma(Z \to H^0\gamma)$ is enhanced by a factor of 100 at $M_{H^0} = 60$ GeV leading to measurable cross sections at LEP [6].

This search extends to any scalar boson decaying like the Higgs boson in (1) and (2).

The large number of Z decays collected with the L3 detector at LEP allows a search for these rare processes to be conducted. This search has been carried out by studying hadronic events with one or two isolated hard photons in the final state. Previous results for these searches from the L3 and the other LEP collaborations are reported in references [8,9]. The results reported in this paper update our previous measurements and are obtained using events collected at center-of-mass energies in the range $91.0 \leq \sqrt{s} \leq 91.5$ GeV from 1991 through 1994 and corresponding to a total integrated luminosity of 96.8 pb^{-1}.

The L3 Detector

The L3 detector consists of a silicon microvertex detector, a central tracking chamber, a high resolution electromagnetic calorimeter composed of BGO crystals, a barrel of scintillation counters, a uranium hadron calorimeter with proportional wire chamber readout, and an accurate muon chamber system. These detectors are installed in a 12 m diameter magnet which provides a solenoidal field of 0.5 T and a toroidal field of 1.2 T. Luminosity is measured with a forward-backward BGO calorimeter on each side of the detector. A detailed description of each detector subsystem and its performance is given in [10, 11].

The electromagnetic calorimeter consists of 10734 BGO crystals divided into a barrel with a polar angle coverage $42^\circ \leq \theta \leq 138^\circ$ and two endcaps corresponding to the polar angle coverage $10^\circ \leq \theta \leq 37^\circ$ and $143^\circ \leq \theta \leq 170^\circ$ For electrons and photons of more than 5 GeV the energy resolution is less than 2% with an angular resolution better than 2 mrad.

The response of the L3 detector is modelled with the GEANT 3.15 detector simulation program [12] which includes the effects of energy loss, multiple scattering and showering in the detector materials and in the beam pipe as well as the time-dependent inefficiencies of the various subdetectors.

Selection of Hadronic Events with Hard Photons

The selection of $e^+e^- \rightarrow$ hadrons events is based on the energy measured in the electromagnetic and hadronic calorimeters.

We measure the total visible energy (E_{vis}) and the energy imbalances parallel ($E_{||}$) and perpendicular ($E_\perp$) to the beam direction. We select an event to be hadronic if it satisfies the following cuts:

- $N_{clusters} > 12$,
- $0.6 < E_{vis}/\sqrt{s} < 1.4$,
- $E_\perp/E_{vis} < 0.4$,
- $|E_{||}|/E_{vis} < 0.4$.

Only clusters with energy greater than 100 MeV have been used. Since the number of clusters is proportional to the number of particles in the event, the cut on $N_{clusters}$ serves to reject low multiplicity events, which are mainly leptonic or two-photon events.

Applying these cuts to 2.2 million fully simulated events, we find that 98% of the hadronic Z decays are accepted. The Monte Carlo hadronic events were generated using JETSET 7.3 [13] with parton shower and string fragmentation. In order to reduce the contribution from initial state radiation we restrict our study to the events produced near the Z peak corresponding to a center-of-mass energy $91.0 \leq \sqrt{s} \leq 91.5$ GeV. We select 2.8 million hadronic events. The photon candidates are selected from the previous event sample by requiring the following criteria on reconstructed clusters in the electromagnetic calorimeter:

- $E_{cluster} > 5$ GeV,
- $17^\circ \leq \theta_\gamma \leq 35^\circ$, or $45^\circ \leq \theta_\gamma \leq 135^\circ$, or $145^\circ \leq \theta_\gamma \leq 163^\circ$,
- no track associated to the cluster.

The cut on the polar angle θ_γ is chosen such that an electromagnetic shower is well contained either in the endcaps or in the barrel. The matching of tracks to electromagnetic clusters is performed in the plane transverse to the beam, by extrapolating the track to the estimated position of the cluster and then measuring the azimuthal separation at this radius.

Most of the photons produced in hadronic Z decays come from fragmentation products, mainly π^0's and η's decaying into photons. To reduce significantly this contamination we isolate the photon candidates by requiring no other electromagnetic cluster with an energy above 40 MeV in a cone of half-angle 15° around the candidate direction.

To improve the neutral hadron rejection, we also use a neural network classifier [14] to discriminate single photon showers from multi-photon showers produced in the electromagnetic calorimeter. This cut accepts 90% of the photons while rejecting from 55% up to 70% of the neutral hadrons for 20 GeV clusters; the rejection rate is higher in the BGO barrel (65% – 70%) than in the endcaps (55% – 65%) due to the more complex endcap geometry.

From the 2.8 million hadronic events studied, 11538 events with 11567 photon candidates pass these selection criteria. According to Monte Carlo simulations, approximately 77% of the selected photon candidates originate from final state radiation, 11% from initial state radiation and 12% are due to neutral hadrons faking a single photon. These three background sources are irreducible.

Search for a Narrow Resonance

The signature for process (1) is a monochromatic photon accompanied by hadrons. Since the Z produced in e^+e^- collisions at LEP is at rest, the energy (E_γ) of the photon is determined by the mass of the resonance ($M_{\rm H}$) using the following formula:

$$M_{\rm H}^2 = M_{\rm recoil}^2 = m_{\rm Z}^2 - 2E_\gamma m_{\rm Z}, \tag{3}$$

where $M_{\rm recoil}$ denotes the mass of the recoiling hadronic system and $m_{\rm Z}$ is the Z mass. The very good energy resolution of the BGO calorimeter can be used to determine the mass of the resonance. This translates into a mass resolution ranging from 0.6% for a 80 GeV resonance mass up to 25% for a 20 GeV mass.

We use the PYTHIA 5.6 event generator [15] to simulate the process (1) for the Higgs mass values of 30, 40, 60 and 80 GeV. The H^0 was assumed to decay isotropically. The events were passed through the full detector simulation. The selection efficiencies for signal events obtained with the four mass values with an overlaid fit of a second order polynomial are shown in Figure 2. The efficiency varies from 60% to 77%.

The dominant systematic error in determining the efficiency is due to hadronization uncertainties. This is estimated by using a different fragmentation scheme, based on cluster fragmentation implemented in the HERWIG QCD model [16]. We estimate the uncertainty as the difference between the two model predictions for selecting $q\bar{q}\gamma$ events with the previous cuts. This gives an error of about 2% on the efficiency. Other systematic effects can be neglected.

Process (1) would appear as a peak in the $M_{\rm recoil}$ distribution. The background is estimated from the data so as not to introduce systematic effects from uncertainties in Monte Carlo expectations: an exponential plus a second order polynomial is fit, see Figure 3. Such a fit, performed over a mass range much wider than the expected signal width, would not be affected by the possible presence of a resonance peak.

We have searched for a peak in the photon energy spectrum by scanning the distribution with a mass window defined by

$$\Delta M = \frac{\sigma(E_\gamma)}{E_\gamma}\frac{(m_{\mathrm{Z}}^2 - M_{\mathrm{H}}^2)}{M_{\mathrm{H}}}. \quad (4)$$

The width of the mass window is determined by the energy resolution of the electromagnetic calorimeter $\sigma(E_\gamma)/E_\gamma$, which has been conservatively set to 2%. For a Higgs mass centered inside a bin, about 68% of the signal events will be contained within such a window. For each bin, we compare the observed number of events to the prediction of the background fit.

The analysis has been performed separately for Higgs mass values ranging from 20 to 60 GeV and from 60 to 80 GeV. This is due to the fact that for low Higgs mass values (high photon energies) the width of the mass window determined from eq. (4) is larger than for higher Higgs mass values. In addition, the energy distribution of photons decreases almost exponentially, therefore, in order to perform a reliable fit for the background, a larger bin size is needed for higher photon energies (lower Higgs masses). For the M_{recoil} spectrum we therefore use 0.7 GeV bins for $M_{\mathrm{H^0}} < 60$ GeV and 0.3 GeV bins for $M_{\mathrm{H^0}} > 60$ GeV. The M_{recoil} spectrum together with the fit for the background is shown in Figure 3.

No evidence for a Higgs signal is visible through this process. The 95% C.L. upper limit for the cross section $\sigma(\mathrm{e^+e^-} \to \mathrm{H^0}\gamma) \times \mathrm{Br}(\mathrm{H^0} \to \mathrm{q\bar{q}})$ is presented in Figure 4 as a function of the $\mathrm{H^0}$ mass together with predictions from different models. In calculating the upper limit we have conservatively lowered the efficiency by one standard deviation. The limit is one to two orders of magnitude higher than the Standard Model expectation while it is two to three times the maximum possible MSSM value for a Higgs mass below 50 GeV. As a result of this search it is possible to exclude combinations of the coefficients f_i in the model involving the dimension-six Lagrangian which give cross sections larger than our obtained upper limit. This search also excludes the Strongly Coupled Standard Model (SCSM) if the scale factor Λ is less than 100 GeV.

Search for a Scalar Boson Decaying Into Two Photons

The expected signature for process (2) is two isolated energetic photons accompanied by hadrons. The event sample is obtained from the previous one by requiring at least two photon candidates with an energy greater than 10 GeV. No events with three photon candidates pass these cuts. The photon energy distribution of the Monte Carlo $\mathrm{H^0}$ signal, together with the distribution obtained from data before the cut is applied, is shown in Figure 5. The corresponding clusters should be separated by at least 40° in space angle and should be separated from the nearest hadronic jet by more than than 30°. The jets are reconstructed using the JADE [17] algorithm with y_{cut}=0.05 excluding the isolated photon candidates from the reconstruction. The last two cuts have been optimised using Monte Carlo events for hadronic Z decays and for the reaction under study.

From the complete data sample we select 7 events. The main characteristics of these events are summarised in Table 1.

Process (2) for the five Higgs mass values 20, 30, 40, 50 and 60 GeV has been simulated as before. The events have been passed through the full L3 detector simulation to determine the selection efficiencies which are shown in Figure 6 with an overlaid fit of a second order polynomial. The selection efficiencies vary between 16% at 20 GeV and 34% at 50 GeV. We use the same systematic uncertainty on the fragmentation process as in the $\mathrm{Z} \to \mathrm{H^0}\gamma$ case.

The $\gamma\gamma$ invariant mass resolution is 3% for $M_{\mathrm{H^0}} = 10$ GeV and 2% for $M_{\mathrm{H^0}} > 30$ GeV with a BGO energy resolution of 2%.

$E_{\gamma,1}$ (GeV)	$E_{\gamma,2}$ (GeV)	$\Delta\Phi'$ (deg)	$M_{\gamma\gamma}$ (GeV)
29.1	15.3	97.5	31.7
35.4	26.4	132.8	56.0
10.4	16.5	135.6	24.3
31.9	38.7	147.4	67.5
22.4	14.4	119.3	31.0
29.6	11.0	84.4	24.3
13.3	36.9	125.7	39.4

Table 1: Events with two isolated photon candidates. $E_{\gamma,1}$ and $E_{\gamma,2}$ denote the energies of the photons, $\Delta\Phi'$ is the space angle between the photon directions and $M_{\gamma\gamma}$ is the invariant mass of the photon pair.

The same selection applied to the 2.16 million hadronic Z decays generated with Monte Carlo retains only two events. It should be noticed that the JETSET prediction for the rate of final state photons and isolated neutral hadrons in hadronic events is lower than experimentally observed, the discrepancy being 15%–29% [14]. Due to this discrepancy, the Monte Carlo background for $\mathrm{q\bar{q}}\gamma\gamma$ events is underestimated. We have therefore estimated the background for the $\gamma\gamma$ invariant mass distribution by using the experimentally determined photon energy distribution in $\mathrm{q\bar{q}}\gamma$ events. We assume that the two energetic photons in a hadronic event are produced independently of each other. The $\gamma\gamma$ invariant mass distribution for the background obtained following this method is in good agreement with the observed $\gamma\gamma$ invariant mass distribution, the agreement being independent of the event selection criteria. The estimated number of background events corresponding to the number of hadronic events in the data is 4.8. However, in calculating the upper limit for the corresponding cross section, this background can be neglected since the corresponding events are distributed over several $\gamma\gamma$ invariant mass bins. The background contribution to the cross section upper limit is estimated to be of the order of 3% and is neglected.

No clear signal for $\mathrm{H^0} \to \gamma\gamma$ is seen. The 95% C.L. upper limit for the cross section $\sigma(\mathrm{e^+e^-} \to \mathrm{H^0} + \mathrm{hadrons}) \times \mathrm{Br}(\mathrm{H^0} \to \gamma\gamma)$ and its comparison to different theoretical predictions is presented in Figure 7 as a function of the $\mathrm{H^0}$ mass. In calculating the upper limit we have conservatively lowered the efficiency by one standard deviation.

The limit is more than two orders of magnitude higher than the Standard Model expectation. As for the other search it is possible to exclude the combinations of coefficients f_i in the model involving a dimension-six Lagrangian which give cross sections higher than our upper limit. The Strongly Coupled Standard Model is excluded for the scale factor Λ less than 100 GeV.

Conclusion

No evidence of a Higgs boson produced in the reactions $\mathrm{e^+e^-} \to \mathrm{Z} \to \mathrm{H^0}\gamma$, $\mathrm{H^0} \to \mathrm{q\bar{q}}$ and $\mathrm{e^+e^-} \to \mathrm{Z} \to \mathrm{H^0Z^*}$, $\mathrm{H^0} \to \gamma\gamma$, $\mathrm{Z^*} \to \mathrm{q\bar{q}}$ is observed in the data collected at LEP with the L3 detector during the period from 1991 through 1994 with an integrated luminosity of 96.8 $\mathrm{pb^{-1}}$.

We set upper limits on cross sections for these two processes. Our 95% C.L. limit for $\sigma(e^+e^- \to H^0\gamma) \times \mathrm{Br}(H^0 \to q\bar{q})$ is in the range 0.3 to 1.0 pb for Higgs mass values between 20 and 80 GeV.

The 95% C.L. upper limit on the cross section $\sigma(e^+e^- \to H^0 + \mathrm{hadrons}) \times \mathrm{Br}(H^0 \to \gamma\gamma)$ is in the range 0.1 to 0.3 pb for Higgs mass values between 20 and 70 GeV.

Models predicting large enhancement of these processes with respect to the Standard Model are excluded in the mass range 20 GeV $\leq M_{H^0} \leq$ 80 GeV. The two measured limits exclude combinations of the coefficients f_i in the model involving a dimension-six Lagrangian which give cross sections higher than our measured limits. Our search also excludes the Strongly Coupled Standard Model if the scale factor Λ is less than 100 GeV.

This study improves our previous limits [8] by one order of magnitude. The results obtained can be extended to any neutral scalar boson decaying into the same final states as the Higgs boson.

Acknowledgements

We wish to express our gratitude to the CERN accelerator divisions for the excellent performance of the LEP machine. We acknowledge with appreciation the effort of all engineers, technicians and support staff who have participated in the construction and maintenance of this experiment. Those of us who are not from member states thank CERN for its hospitality and help.

References

[1] S. L. Glashow, Nucl. Phys. **22** (1961) 579;
S. Weinberg, Phys. Rev. Lett. **19** (1967) 1264;
A. Salam, Elementary Particle Theory, Ed. N. Svartholm, Stockholm, "Almquist and Wiksell" (1968) 367.

[2] P. W. Higgs, Phys. Lett. **12** (1964) 132, Phys. Rev. Lett. **13** (1964) 508, Phys. Rev. **145** (1966) 1156;
F. Englert, R. Brout, Phys. Rev. Lett. **13** (1964) 321.

[3] G. Gamberini, G. F. Giudice, G. Ridolfi, Nucl. Phys. **B292** (1987) 237.

[4] R. Bates, John N. Ng, P. Kalyniak, Phys. Rev. **D34** (1986) 172.

[5] K. Hagiwara, R. Szalapski, D. Zeppenfeld, Phys. Lett. **B318** (1993) 155.

[6] D. W. Düsedau, J. Wudka, Phys. Lett. **B180** (1986) 290.

[7] F. M. Renard, Phys. Lett. **B126** (1983) 59.

[8] L3 Collab., O. Adriani *et al.*, Phys. Lett. **B292** (1992) 472.

[9] ALEPH Collab., D. Buskulic *et al.*, Phys. Lett. **B308** (1993) 425.
DELPHI Collab., P. Abreu *et al.*, Z. Phys. **C53** (1992) 555.
OPAL Collab., P. Acton *et al.*, Phys. Lett. **B311** (1993) 391.

OPAL Collab., G. Alexander *et al.*, Preprint CERN-PPE/95-193, Submitted to Z. Phys. C.

[10] L3 Collab., O. Adriani *et al.*, Phys. Rep. **236** (1993) 1.

[11] L3 Collab., B. Adeva *et al.*, Nucl. Inst. Meth. **A289** (1990) 35;
L3 Collab., M. Acciarri *et al.*, Nucl. Inst. Meth. **A351** (1994) 300.

[12] R. Brun *et al.*, "GEANT 3", CERN DD/EE/84-1 (Revised), September 1987.
The GHEISHA program (H. Fesefeldt, RWTH Aachen Report PITHA 85/02 (1985)) is used to simulate hadronic interactions.

[13] T. Sjöstrand, Comp. Phys. Comm. **39** (1986) 347;
T. Sjöstrand and M. Bengtsson, Comp. Phys. Comm. **43** (1987) 367.

[14] D. Kirkby, A Study of Final-State Radiation in Hadronic Z Decays, Ph.D Thesis, California Institute of Technology (1995) unpublished.

[15] H.-U. Bengtsson, T. Sjöstrand, Comp. Phys. Comm. **46** (1987) 43.

[16] G. Marchesini and B. Webber, Nucl. Phys. **B310** (1988) 461;
I. G. Knowles, Nucl. Phys. **B310** (1988) 571;
G. Marchesini *et al.*, Comp. Phys. Comm. **67** (1992) 465.

[17] JADE Collab., W. Bartel *et al.*, Z. Phys. **C33** (1986) 23;
JADE Collab., S. Bethke *et al.*, Phys. Lett. **B213** (1988) 235.

The L3 Collaboration:

M.Acciarri[28] A.Adam[47] O.Adriani[17] M.Aguilar-Benitez[27] S.Ahlen[11] B.Alpat[35] J.Alcaraz[27] G.Alemanni[23] J.Allaby[18] A.Aloisio[30] G.Alverson[12] M.G.Alviggi[30] G.Ambrosi[20] H.Anderhub[50] V.P.Andreev[39] T.Angelescu[13] D.Antreasyan[9] A.Arefiev[29] T.Azemoon[3] T.Aziz[10] P.Bagnaia[38] L.Baksay[45] R.C.Ball[3] S.Banerjee[10] K.Banicz[47] R.Barillère[18] L.Barone[38] P.Bartalini[35] A.Baschirotto[28] M.Basile[9] R.Battiston[35] A.Bay[23] F.Becattini[17] U.Becker[16] F.Behner[50] J.Berdugo[27] P.Berges[16] B.Bertucci[18] B.L.Betev[50] M.Biasini[18] A.Biland[50] G.M.Bilei[35] J.J.Blaising[18] S.C.Blyth[36] G.J.Bobbink[2] R.Bock[1] A.Böhm[1] B.Borgia[38] A.Boucham[4] D.Bourilkov[50] M.Bourquin[20] D.Boutigny[4] E.Brambilla[16] J.G.Branson[41] V.Brigljevic[50] I.C.Brock[36] A.Buijs[46] A.Bujak[47] J.D.Burger[16] W.J.Burger[20] J.Busenitz[45] A.Buytenhuijs[32] X.D.Cai[19] M.Campanelli[50] M.Capell[16] G.Cara Romeo[9] M.Caria[35] G.Carlino[4] A.M.Cartacci[17] J.Casaus[27] G.Castellini[17] R.Castello[28] F.Cavallari[38] N.Cavallo[30] C.Cecchi[20] M.Cerrada[27] F.Cesaroni[24] M.Chamizo[27] A.Chan[52] Y.H.Chang[52] U.K.Chaturvedi[19] M.Chemarin[26] A.Chen[52] G.Chen[7] G.M.Chen[7] H.F.Chen[21] H.S.Chen[7] M.Chen[16] G.Chiefari[30] C.Y.Chien[5] M.T.Choi[44] L.Cifarelli[40] F.Cindolo[9] C.Civinini[17] I.Clare[16] R.Clare[16] H.O.Cohn[33] G.Coignet[4] A.P.Colijn[2] N.Colino[27] S.Costantini[38] F.Cotorobai[13] B.de la Cruz[27] A.Csilling[14] T.S.Dai[16] R.D'Alessandro[17] R.de Asmundis[30] H.De Boeck[32] A.Degré[4] K.Deiters[48] P.Denes[37] F.DeNotaristefani[38] D.DiBitonto[45] M.Diemoz[38] D.van Dierendonck[2] F.Di Lodovico[50] C.Dionisi[38] M.Dittmar[50] A.Dominguez[41] A.Doria[30] I.Dorne[4] M.T.Dova[19,♯] E.Drago[30] D.Duchesneau[4] P.Duinker[2] I.Duran[42] S.Dutta[10] S.Easo[35] Yu.Efremenko[33] H.El Mamouni[26] A.Engler[36] F.J.Eppling[16] F.C.Erné[2] J.P.Ernenwein[26] P.Extermann[20] M.Fabre[48] R.Faccini[38] S.Falciano[38] A.Favara[17] J.Fay[26] M.Felcini[50] C.Furetta[28] T.Ferguson[36] D.Fernandez[27] F.Ferroni[38] H.Fesefeldt[1] E.Fiandrini[35] J.H.Field[20] F.Filthaut[36] P.H.Fisher[16] G.Forconi[16] L.Fredj[20] K.Freudenreich[50] Yu.Galaktionov[29,16] S.N.Ganguli[10] S.S.Gau[12] S.Gentile[38] J.Gerald[5] N.Gheordanescu[13] S.Giagu[38] S.Goldfarb[23] J.Goldstein[11] Z.F.Gong[21] A.Gougas[5] G.Gratta[34] M.W.Gruenewald[8] V.K.Gupta[37] A.Gurtu[10] L.J.Gutay[47] K.Hangarter[1] B.Hartmann[1] A.Hasan[31] T.Hebbeker[8] A.Hervé[18] W.C.van Hoek[32] H.Hofer[50] H.Hoorani[20] S.R.Hou[52] G.Hu[19] M.M.Ilyas[19] V.Innocente[18] H.Janssen[4] B.N.Jin[7] L.W.Jones[3] P.de Jong[16] I.Josa-Mutuberria[27] A.Kasser[23] R.A.Khan[19] Yu.Kamyshkov[33] P.Kapinos[49] J.S.Kapustinsky[25] Y.Karyotakis[4] M.Kaur[19,◇] M.N.Kienzle-Focacci[20] D.Kim[5] J.K.Kim[44] S.C.Kim[44] Y.G.Kim[44] W.W.Kinnison[25] A.Kirkby[34] D.Kirkby[34] J.Kirkby[18] D.Kiss[14] W.Kittel[32] A.Klimentov[16,29] A.C.König[32] I.Korolko[29] V.Koutsenko[16,29] A.Koulbardis[39] R.W.Kraemer[36] T.Kramer[16] W.Krenz[1] H.Kuijten[32] A.Kunin[16,29] P.Ladron de Guevara[27] G.Landi[17] C.Lapoint[16] K.Lassila-Perini[50] P.Laurikainen[22] M.Lebeau[18] A.Lebedev[16] P.Lebrun[26] P.Lecomte[50] P.Lecoq[18] P.Le Coultre[50] J.S.Lee[44] K.Y.Lee[44] C.Leggett[3] J.M.Le Goff[18] R.Leiste[49] M.Lenti[17] E.Leonardi[38] P.Levtchenko[39] C.Li[21] E.Lieb[49] W.T.Lin[52] F.L.Linde[2,18] L.Lista[30] Z.A.Liu[7] W.Lohmann[49] E.Longo[38] W.Lu[34] Y.S.Lu[7] K.Lübelsmeyer[1] C.Luci[38] D.Luckey[16] L.Ludovici[38] L.Luminari[38] W.Lustermann[48] W.G.Ma[21] A.Macchiolo[17] M.Maity[10] G.Majumder[10] L.Malgeri[38] A.Malinin[29] C.Maña[27] S.Mangla[10] P.Marchesini[50] A.Marin[11] J.P.Martin[26] F.Marzano[38] G.G.G.Massaro[2] K.Mazumdar[10] D.McNally[18] S.Mele[30] L.Merola[30] M.Meschini[17] W.J.Metzger[32] M.von der Mey[1] Y.Mi[23] A.Mihul[13] A.J.W.van Mil[32] G.Mirabelli[38] J.Mnich[18] B.Monteleoni[17] R.Moore[3] S.Morganti[38] R.Mount[34] S.Müller[1] F.Muheim[20] E.Nagy[14] S.Nahn[16] M.Napolitano[30] F.Nessi-Tedaldi[50] H.Newman[34] A.Nippe[1] H.Nowak[49] G.Organtini[38] R.Ostonen[22] D.Pandoulas[1] S.Paoletti[38] P.Paolucci[30] H.K.Park[36] G.Pascale[38] G.Passaleva[17] S.Patricelli[30] T.Paul[12] M.Pauluzzi[35] C.Paus[1] F.Pauss[50] D.Peach[18] Y.J.Pei[1] S.Pensotti[28] D.Perret-Gallix[4] S.Petrak[8] A.Pevsner[5] D.Piccolo[30] M.Pieri[17] J.C.Pinto[36] P.A.Piroué[37] E.Pistolesi[17] V.Plyaskin[29] M.Pohl[50] V.Pojidaev[29,17] H.Postema[16] N.Produit[20] R.Raghavan[10] G.Rahal-Callot[50] P.G.Rancoita[28] M.Rattaggi[28] G.Raven[41] P.Razis[31] K.Read[33] D.Ren[50] M.Rescigno[38] S.Reucroft[12] T.van Rhee[46] S.Riemann[49] B.C.Riemers[47] K.Riles[3] O.Rind[3] S.Ro[44] A.Robohm[50] J.Rodin[16] F.J.Rodriguez[27] B.P.Roe[3] S.Röhner[1] L.Romero[27] S.Rosier-Lees[4] Ph.Rosselet[23] W.van Rossum[46] S.Roth[1] J.A.Rubio[18] H.Rykaczewski[50] J.Salicio[18] E.Sanchez[27] A.Santocchia[35] M.E.Sarakinos[22] S.Sarkar[10] M.Sassowsky[1] G.Sauvage[4] C.Schäfer[1] V.Schegelsky[39] S.Schmidt-Kaerst[1] D.Schmitz[1] P.Schmitz[1] M.Schneegans[4] B.Schoeneich[49] N.Scholz[50] H.Schopper[51] D.J.Schotanus[32] J.Schwenke[1] G.Schwering[1] C.Sciacca[30] D.Sciarrino[20] J.C.Sens[52] L.Servoli[35] S.Shevchenko[34] N.Shivarov[43] V.Shoutko[29] J.Shukla[25] E.Shumilov[29] T.Siedenburg[1] D.Son[44] A.Sopczak[49] V.Soulimov[30] B.Smith[16] P.Spillantini[17] M.Steuer[16] D.P.Stickland[37] F.Sticozzi[16] H.Stone[37] B.Stoyanov[43] A.Straessner[1] K.Strauch[15] K.Sudhakar[10] G.Sultanov[19] L.Z.Sun[21] G.F.Susinno[20] H.Suter[50] J.D.Swain[19] X.W.Tang[7] L.Tauscher[6] L.Taylor[12] Samuel C.C.Ting[16] S.M.Ting[16] F.Tonisch[49] M.Tonutti[1] S.C.Tonwar[10] J.Tóth[14] A.Tsaregorodtsev[39] C.Tully[37] H.Tuchscherer[45] K.L.Tung[7] J.Ulbricht[50] U.Uwer[18] E.Valente[38] R.T.Van de Walle[32] G.Vesztergombi[14] I.Vetlitsky[29] G.Viertel[50] M.Vivargent[4] R.Völkert[49] H.Vogel[36] H.Vogt[49] I.Vorobiev[29] A.A.Vorobyov[39] An.A.Vorobyov[39] A.Vorvolakos[31] M.Wadhwa[6] W.Wallraff[1] J.C.Wang[16] X.L.Wang[21] Y.F.Wang[16] Z.M.Wang[21] A.Weber[1] F.Wittgenstein[18] S.X.Wu[19] S.Wynhoff[1] J.Xu[11] Z.Z.Xu[21] B.Z.Yang[21] C.G.Yang[7] X.Y.Yao[7] J.B.Ye[21] S.C.Yeh[52] J.M.You[36] C.Zaccardelli[34] An.Zalite[39] P.Zemp[50] Y.Zeng[1] Z.Zhang[7] Z.P.Zhang[21] B.Zhou[11] Y.Zhou[3] G.Y.Zhu[7] R.Y.Zhu[34] A.Zichichi[9,18,19]

1 I. Physikalisches Institut, RWTH, D-52056 Aachen, FRG[§]
III. Physikalisches Institut, RWTH, D-52056 Aachen, FRG[§]
2 National Institute for High Energy Physics, NIKHEF, and University of Amsterdam, NL-1009 DB Amsterdam, The Netherlands
3 University of Michigan, Ann Arbor, MI 48109, USA
4 Laboratoire d'Annecy-le-Vieux de Physique des Particules, LAPP,IN2P3-CNRS, BP 110, F-74941 Annecy-le-Vieux CEDEX, France
5 Johns Hopkins University, Baltimore, MD 21218, USA
6 Institute of Physics, University of Basel, CH-4056 Basel, Switzerland
7 Institute of High Energy Physics, IHEP, 100039 Beijing, China
8 Humboldt University, D-10099 Berlin, FRG[§]
9 INFN-Sezione di Bologna, I-40126 Bologna, Italy
10 Tata Institute of Fundamental Research, Bombay 400 005, India
11 Boston University, Boston, MA 02215, USA
12 Northeastern University, Boston, MA 02115, USA
13 Institute of Atomic Physics and University of Bucharest, R-76900 Bucharest, Romania
14 Central Research Institute for Physics of the Hungarian Academy of Sciences, H-1525 Budapest 114, Hungary[‡]
15 Harvard University, Cambridge, MA 02139, USA
16 Massachusetts Institute of Technology, Cambridge, MA 02139, USA
17 INFN Sezione di Firenze and University of Florence, I-50125 Florence, Italy
18 European Laboratory for Particle Physics, CERN, CH-1211 Geneva 23, Switzerland
19 World Laboratory, FBLJA Project, CH-1211 Geneva 23, Switzerland
20 University of Geneva, CH-1211 Geneva 4, Switzerland
21 Chinese University of Science and Technology, USTC, Hefei, Anhui 230 029, China
22 SEFT, Research Institute for High Energy Physics, P.O. Box 9, SF-00014 Helsinki, Finland
23 University of Lausanne, CH-1015 Lausanne, Switzerland
24 INFN-Sezione di Lecce and Universitá Degli Studi di Lecce, I-73100 Lecce, Italy
25 Los Alamos National Laboratory, Los Alamos, NM 87544, USA
26 Institut de Physique Nucléaire de Lyon, IN2P3-CNRS,Université Claude Bernard, F-69622 Villeurbanne, France
27 Centro de Investigaciones Energeticas, Medioambientales y Tecnologicas, CIEMAT, E-28040 Madrid, Spain[♭]
28 INFN-Sezione di Milano, I-20133 Milan, Italy
29 Institute of Theoretical and Experimental Physics, ITEP, Moscow, Russia
30 INFN-Sezione di Napoli and University of Naples, I-80125 Naples, Italy
31 Department of Natural Sciences, University of Cyprus, Nicosia, Cyprus
32 University of Nymegen and NIKHEF, NL-6525 ED Nymegen, The Netherlands
33 Oak Ridge National Laboratory, Oak Ridge, TN 37831, USA
34 California Institute of Technology, Pasadena, CA 91125, USA
35 INFN-Sezione di Perugia and Universitá Degli Studi di Perugia, I-06100 Perugia, Italy
36 Carnegie Mellon University, Pittsburgh, PA 15213, USA
37 Princeton University, Princeton, NJ 08544, USA
38 INFN-Sezione di Roma and University of Rome, "La Sapienza", I-00185 Rome, Italy
39 Nuclear Physics Institute, St. Petersburg, Russia
40 University and INFN, Salerno, I-84100 Salerno, Italy
41 University of California, San Diego, CA 92093, USA
42 Dept. de Fisica de Particulas Elementales, Univ. de Santiago, E-15706 Santiago de Compostela, Spain
43 Bulgarian Academy of Sciences, Central Laboratory of Mechatronics and Instrumentation, BU-1113 Sofia, Bulgaria
44 Center for High Energy Physics, Korea Advanced Inst. of Sciences and Technology, 305-701 Taejon, Republic of Korea
45 University of Alabama, Tuscaloosa, AL 35486, USA
46 Utrecht University and NIKHEF, NL-3584 CB Utrecht, The Netherlands
47 Purdue University, West Lafayette, IN 47907, USA
48 Paul Scherrer Institut, PSI, CH-5232 Villigen, Switzerland
49 DESY-Institut für Hochenergiephysik, D-15738 Zeuthen, FRG
50 Eidgenössische Technische Hochschule, ETH Zürich, CH-8093 Zürich, Switzerland
51 University of Hamburg, D-22761 Hamburg, FRG
52 High Energy Physics Group, Taiwan, China
§ Supported by the German Bundesministerium für Bildung, Wissenschaft, Forschung und Technologie
‡ Supported by the Hungarian OTKA fund under contract number T14459.
♭ Supported also by the Comisión Interministerial de Ciencia y Tecnología
♯ Also supported by CONICET and Universidad Nacional de La Plata, CC 67, 1900 La Plata, Argentina
◇ Also supported by Panjab University, Chandigarh-160014, India

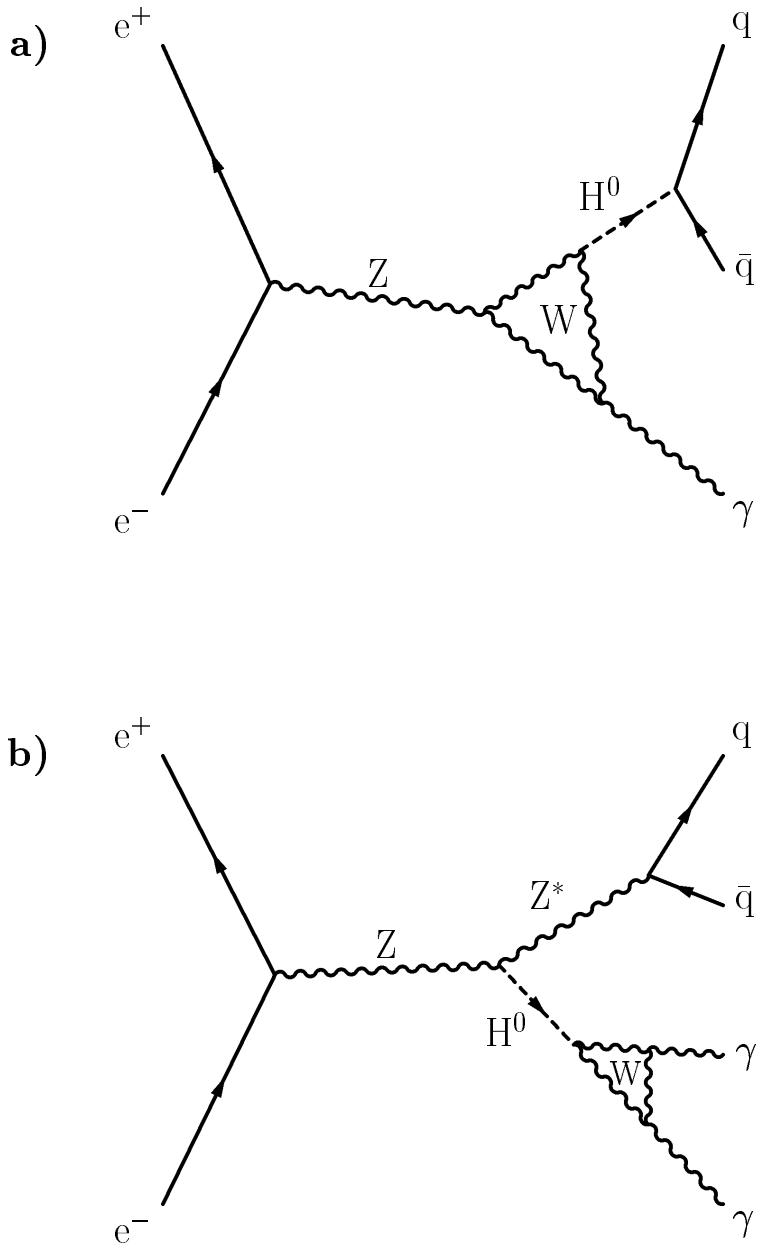

Figure 1: Feynman diagrams for the process (a) $e^+e^- \rightarrow Z \rightarrow H^0\gamma$ with $H^0 \rightarrow q\bar{q}$ and (b) $e^+e^- \rightarrow Z \rightarrow H^0Z^*$ with $H^0 \rightarrow \gamma\gamma$, $Z^* \rightarrow q\bar{q}$. In the Standard Model the Z decay in (a) and the H^0 decay in (b) occur via charged boson or fermion (not shown on the plot) loops.

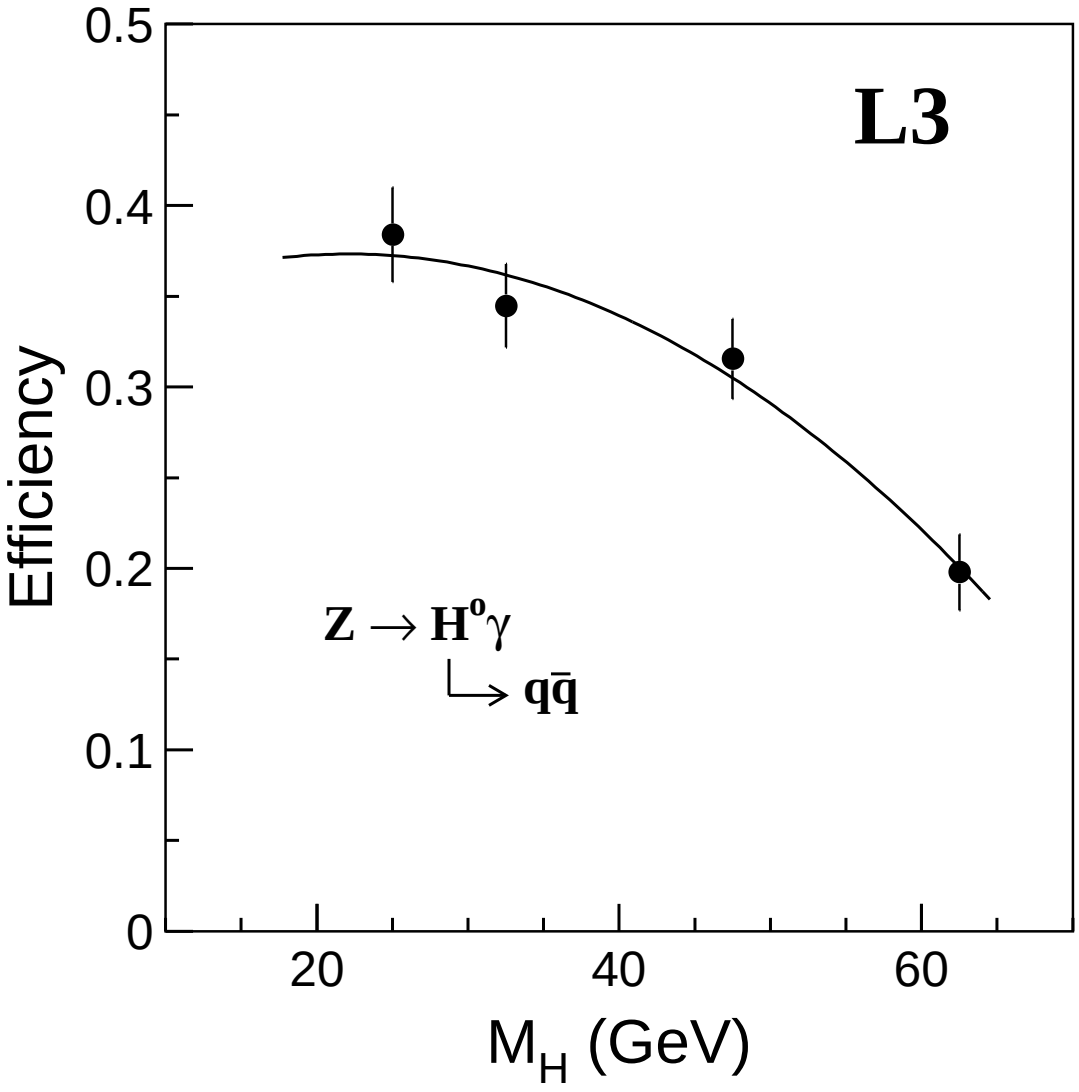

Figure 2: Selection efficiency for the process $Z \rightarrow H^0\gamma$, $H^0 \rightarrow q\bar{q}$ as a function of the Higgs mass. The errors shown include statistical and systematic uncertainties.

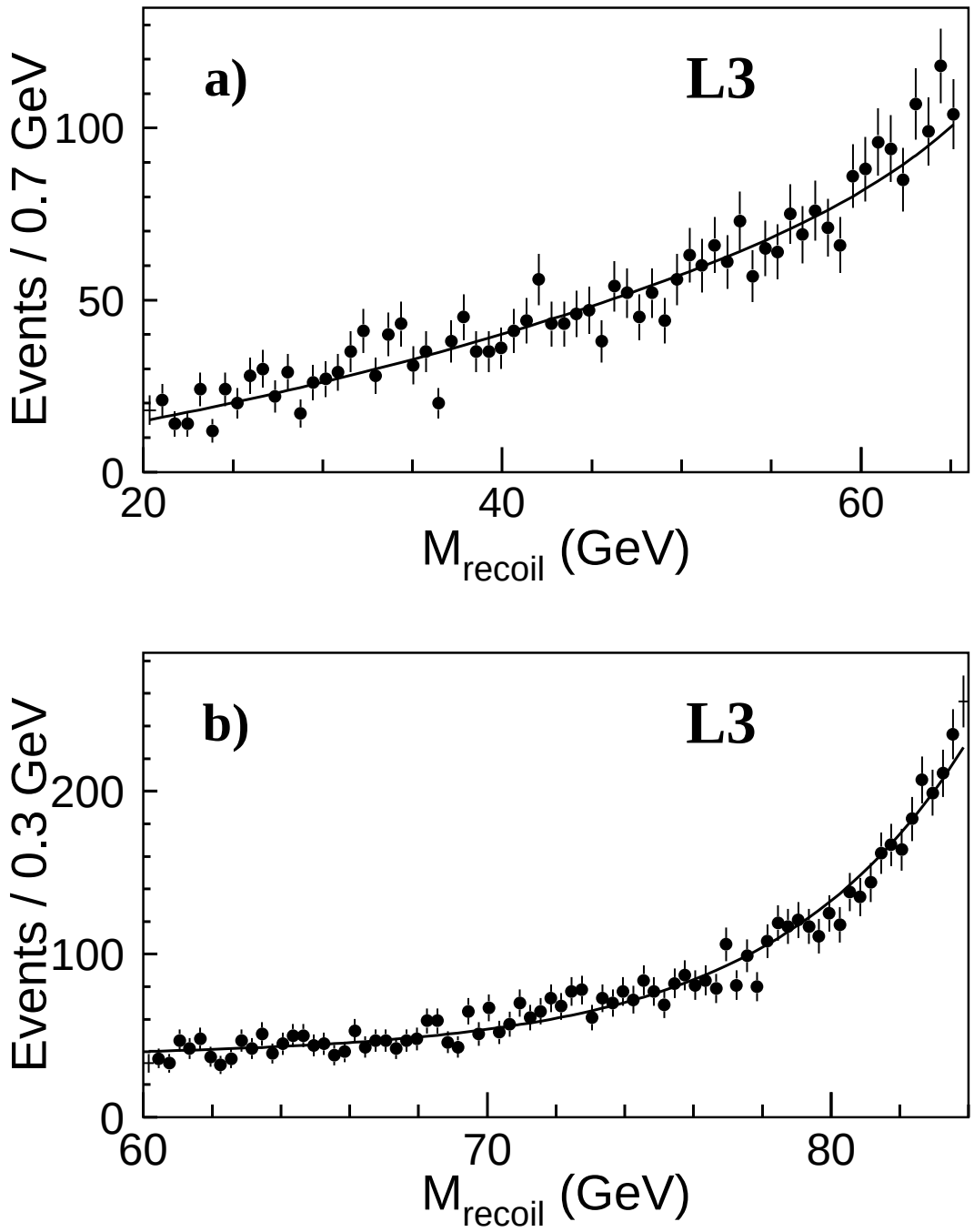

Figure 3: The recoiling hadronic mass spectrum obtained from the photon energy together with a fit for the background for two ranges of mass values (a) $M_{\mathrm{recoil}} < 65$ GeV and (b) $M_{\mathrm{recoil}} > 60$ GeV.

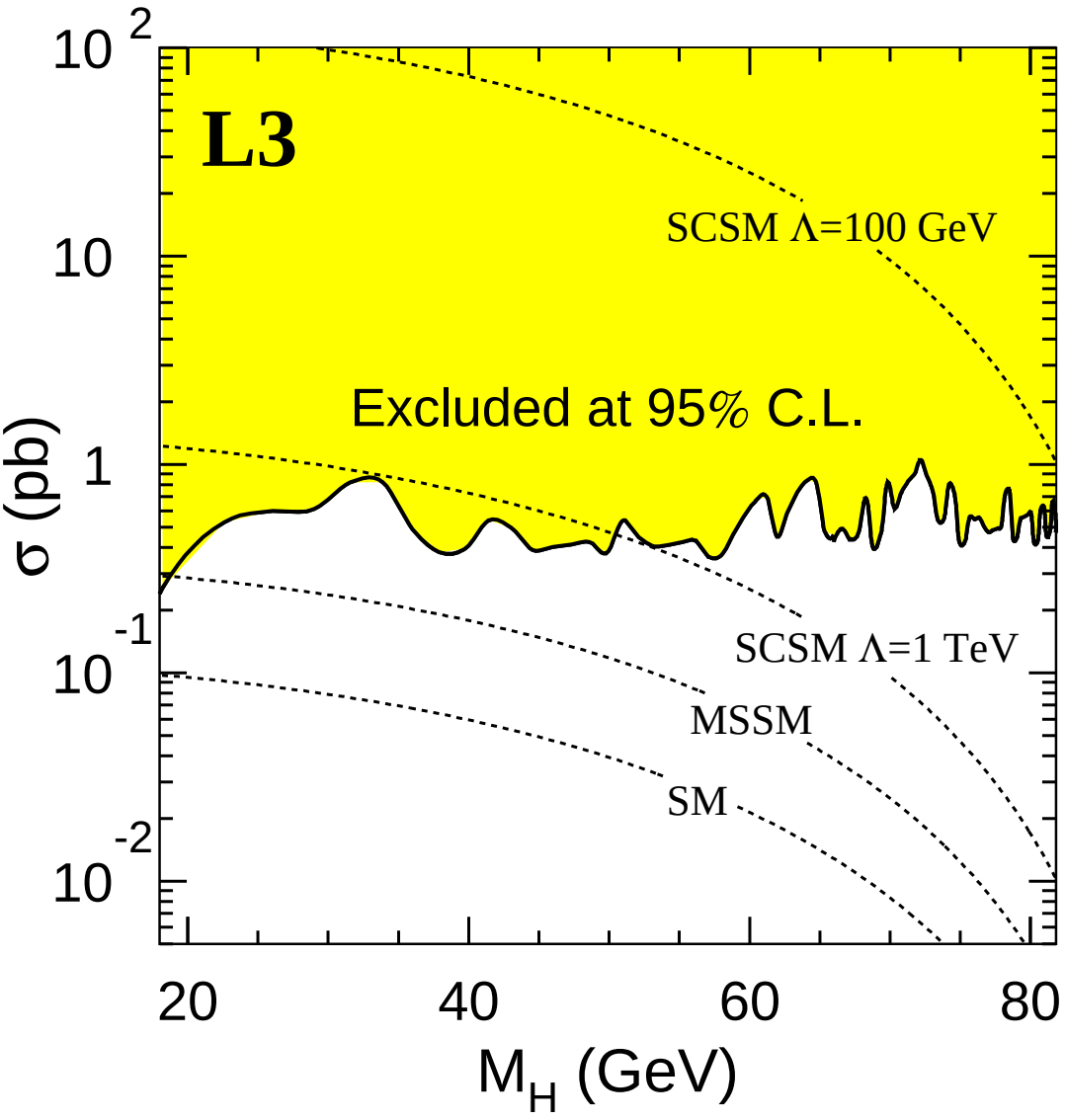

Figure 4: The 95% C.L. upper limit for the cross section $\sigma(e^+e^- \to H^0\gamma) \times Br(H^0 \to q\bar{q})$ together with some theoretical predictions. SM – Standard Model, MSSM – Minimal Supersymmetric Standard Model, SCSM – Strongly Coupled Standard Model. For the MSSM prediction we present the maximal allowed enchancement of the cross section as given in [3]. For the SCSM, the compositeness scale Λ is noted.

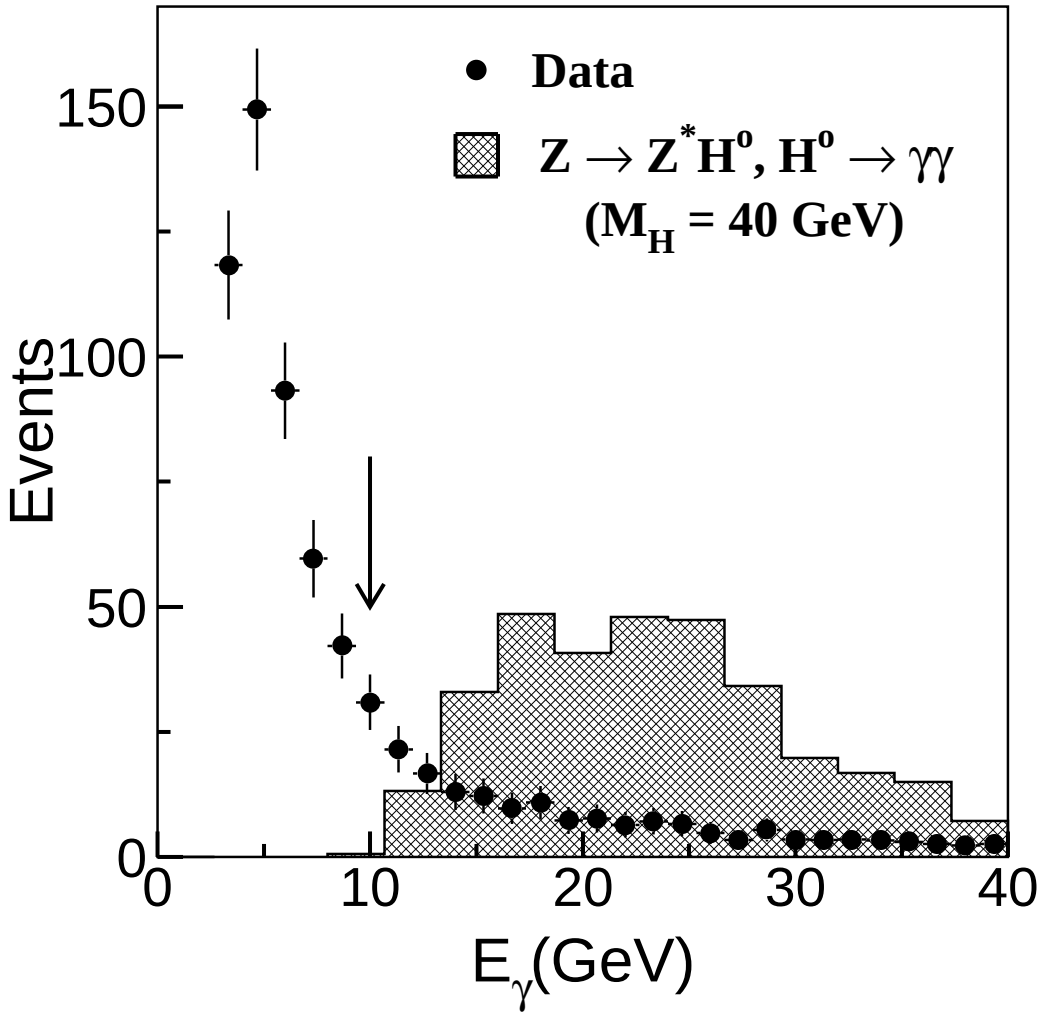

Figure 5: The energy distribution of photon candidates in hadronic events with two or more photons for $M_{\mathrm{H^0}} = 40$ GeV Monte Carlo signal together with the corresponding distribution obtained from data. The arrow corresponds to the cut used. The relative normalization of the distributions is arbitrary.

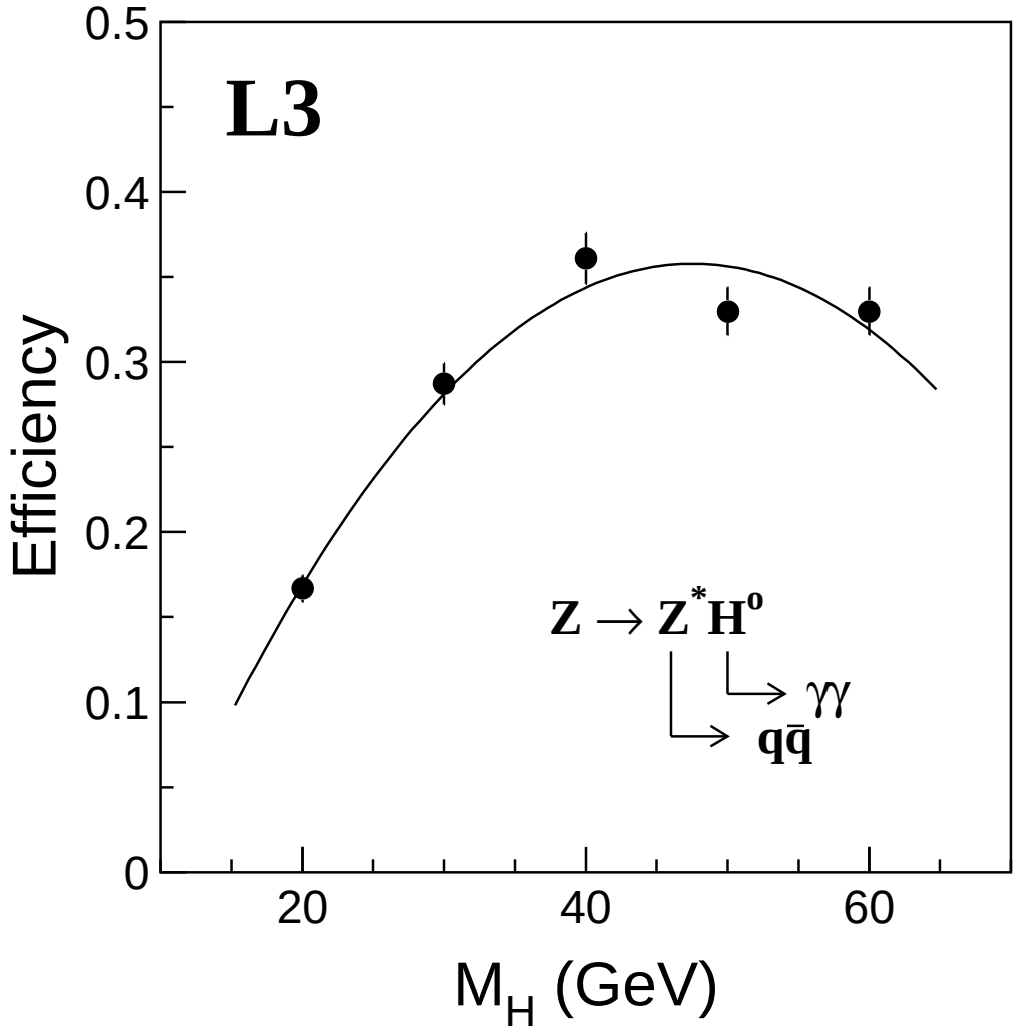

Figure 6: Selection efficiency for the process $Z \rightarrow H^0 q\bar{q}$, $H^0 \rightarrow \gamma\gamma$ as a function of the Higgs mass. The errors shown include statistical and systematic uncertainities.

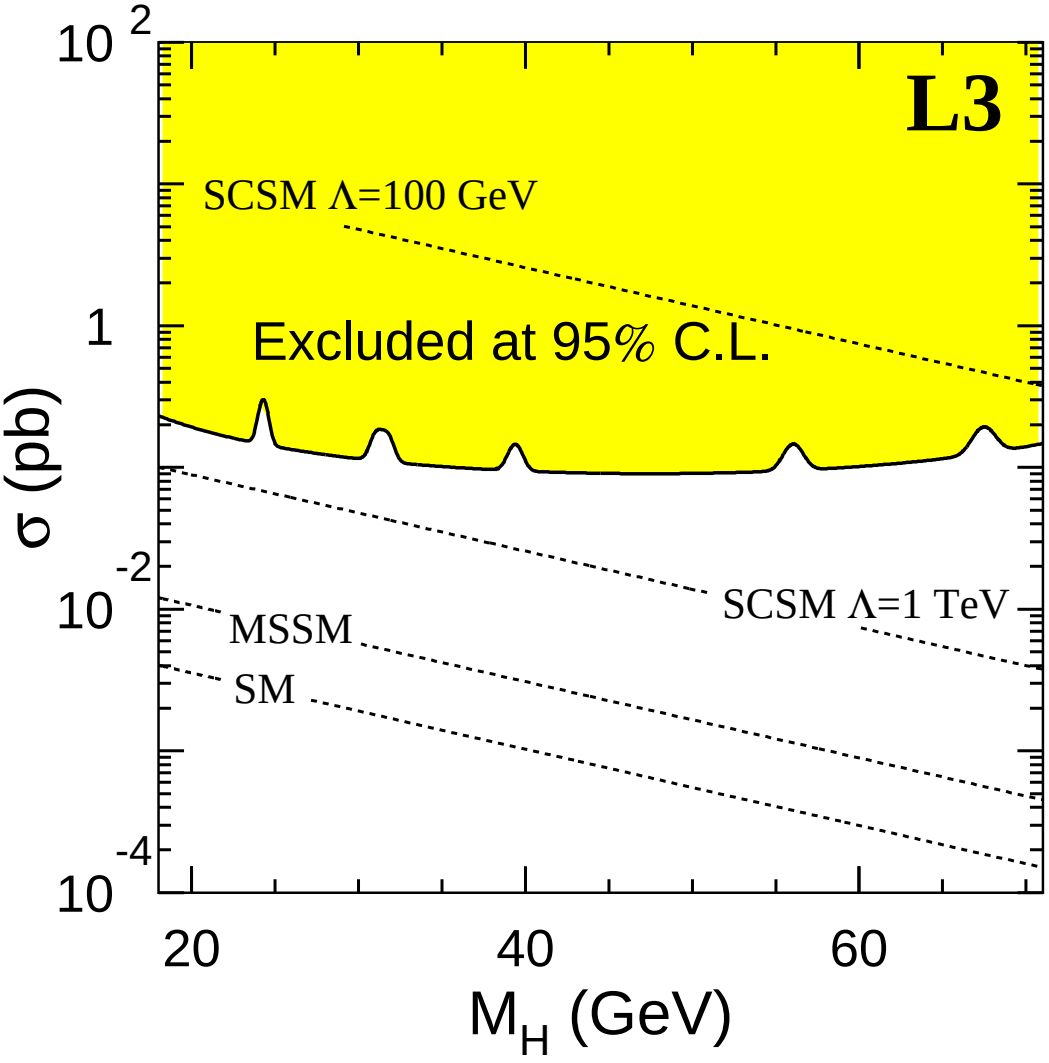

Figure 7: The 95% C.L. upper limit for the cross section $\sigma(e^+e^- \to H^0 + \text{hadrons}) \times \text{Br}(H^0 \to \gamma\gamma)$ together with some theoretical predictions. SM – Standard Model, MSSM – Minimal Supersymmetric Standard Model, SCSM – Strongly Coupled Standard Model. For the MSSM prediction we present the maximal allowed enchancement of the cross section as given in [4]. For the SCSM, the compositeness scale Λ is noted.